

Interactive comment on “Observations and scaling of tidal mass transport across the lower Ganges-Brahmaputra delta plain: implications for delta management and sustainability” by Richard Hale et al.

J. Shaw (Referee)

shaw84@uark.edu

Received and published: 26 October 2018

This study details field observations of tides and sediment transport in the tidal region of the Ganges-Brahmaputra-Megha Delta system. This research is important because of the dearth of direct measurement in this vast system, and provides first insights about how the delta keeps pace with relative sea level rise, context for recent human-induced changes, and a baseline for proposed large scale water projects. The authors characterize tidal range, tidal prism, and sediment transport at a few key sites on primary and secondary distributary channels in the tidal region of the delta. This

manuscript significantly increases our understanding of this system. I have a few questions, but I think that this paper should be published in ESURF after minor revisions. The sediment concentration and transport data are the most important deliverable to me, but I have a hard time summarizing the findings, because they seem contradictory. Point 1: suspended sediment concentration in a secondary channel increases during the wet season by three fold, indicating a fluvial origin (Figure 2). Point 2: Surveys of net sediment discharge in a primary channel collected over all survey days reveal a net import of sediment (Figure 7), which suggests that sediment transport is primarily dependent on net water discharge, which suggests that freshwater arrival is of secondary importance. However, the flux variation here is also about a factor of three or four (Table 1), consistent with the secondary (BR) channel. I encourage the authors to test the hypothesis that the transport of sediments is really controlled by the same thing in both primary (Shibsa) and secondary (BR) channels. I understand that this is difficult to do given the varying data types, but that is a simpler and more tractable explanation.

Minor comments

L258: I think that this is a relatively weak reason to ignore bedload. My intuition is that lots of bed material sand can become suspended under achievable shear velocities and contribute to SSC measurements during velocity maxima, and be transported onto secondary channels or islands if there is enough water discharge. I would say you can neglect bedload if there are no bedforms in your multibeam surveys. Otherwise, I think you just need to say that it could be happening, but that it's likely far less than the suspended component and necessarily neglect it from surveys.

L261: I do not know what "tiling observations" means. Perhaps a quick definition is in order.

L339: It took me a minute to figure out that the tidal prisms you are measuring are from integrating the discharge. I imagine prisms as a space filled, which would be impossible to measure. Consider defining how prisms are found.

L459: Total _annual_ mass transport

L496: I do not understand how sediment moving through the system could be “almost wholly derived from the river mouth,” but that the flux through the five major tidal channels could be estimated as roughly equal to the sediment flux of the main river (L486-487). I would suspect that there could also be significant re-entrainment of continental shelf or island sediments that were once river derived, but have been in the coastal zone for years or maybe far longer than that. I think that the case for re-entrained sediments can't be disproved here.

L555: led to a reduction in tidal prism... assuming no feedbacks to tidal dynamics, correct?

Interactive comment on Earth Surf. Dynam. Discuss., <https://doi.org/10.5194/esurf-2018-66>, 2018.

Printer-friendly version

Discussion paper



Interactive comment on “Observations and scaling of tidal mass transport across the lower Ganges-Brahmaputra delta plain: implications for delta management and sustainability” by Richard Hale et al.

Allison (Referee)

meadallison@tulane.edu

Received and published: 27 November 2018

The Hale et al. manuscript is a fine addition to the very sparse literature on water and sediment dynamics in the Ganges-Brahmaputra coastal zone. I think the paper, which should be published, could be improved in several ways.

1. The dataset is sparse, which is understandable given the difficult logistical conditions to work in this setting. However, absence in particular of CTD cast data synchronous with the OBS cast data, left a number of questions in my mind about the possibilities of

Printer-friendly version

Discussion paper



water column salinity stratification in the channels during the dry season, and sediment stratification and bed storage and or sediment convergence during both studies at slack periods and seasonally. I realize that the authors can't fully address these issues, but I think some of the questions could be allayed by presenting some of the original data—ADCP transects of velocity magnitude, direction and backscatter intensity, and OBS profiles for these example sections. None of this data that is used to calculate fluxes is presented as is, and, seeing some of it would be beneficial to the reader.

2. The methodology is lengthy. If necessary, it could be split off into a supplementary methods section, that would allow greater detail on some of the data manipulations to arrive at fluxes that were only briefly covered in the existing version.

3. I believe some mention of the potential importance of tropical cyclones needs presenting in the intro and discussion. That is, these large events may have an impact on sediment fluxes in the system that may or may not exceed the seasonal and tidal scale processes. Although there is no data presented here, it should be mentioned as a possible and unresolved control in the system.

4. line 166. OBS's do not measure SSC's, they measure turbidity and have to be calibrated. Hence, while the profiler OBS was calibrated as discussed, how did SSC's get derived for the long-term station at Sutarkhali?

5. line 256. This mentions ignoring bedload transport but, what is neglected is sand transport in suspension (bed material load transport). Since water sampling was not done isokinetically (Niskin), this component was missed or undersampled. It appears from the water flux rates (no adcp velocity profiles shown) that the tidal energies are high enough during max ebb and flood to transport sand. I would mention this caveat to be fair about what you are actually measuring (fine flux).

Interactive comment on Earth Surf. Dynam. Discuss., <https://doi.org/10.5194/esurf-2018-66>, 2018.

Dear editors,

We are excited to share with you the revised version of our manuscript. We have carefully considered the referee comments, and respond to each point individually in the following text. On their suggestion, we have streamlined some text for clarity, added an additional figure (Fig. 2), and updated our references to include several recent publications. We thank the referees for their comments, which we think have clarified our findings and strengthened the overall manuscript. Thank you for your consideration.

In Response to R1:

Dear Dr. Shaw, I think your assessment of our major findings is accurate, except that I see no contradiction. In the primary channel, we maintain that tidal stage (i.e., discharge) is the dominant control on suspended sediment concentrations year round, with the introduction of GBM-derived material during the monsoon playing a secondary role. In the smaller channels (e.g., Bhadra), seasonal delivery of new material appears to play a larger role in sediment flux. This introduces the idea of a “discharge threshold” above which seasonal sediment delivery is relatively less important, however future research is required to test this idea.

L258 – Point taken. This sentence was introduced to let the reader know that we are not forgetting about bedload. The revised manuscript will be more explicit.

L261 – Text will be updated to explain that “tiling observations” means repeating the measured time series at 12.4-h increments to improve interpolation/extrapolation accuracy.

L339 – We will make sure to define tidal prisms as the integrated discharge in this context.

L459 – This change will be made.

L496 – We don’t mean to imply that extensive mixing is not happening – quite the opposite. Several studies (e.g., Rogers et al., 2013; Rogers and Overeem, 2017) have demonstrated the presence of a weak, excess-⁷Be signal in sediment accumulating on the mangrove platform during the monsoon season, with mixing/dilution offered as one potential explanation. This comparison was intended to provide the reader with a sense of scale. We have reworded to be more clear about our intended meaning.

L555 – In this case, the “volume reduction” refers to poldered area that would have been flooded by the Shibsra and its distributaries, multiplied by a characteristic flooding depth. We have reworded this as “reduction or redistribution” to clarify.

In response to R2:

Dear Dr. Allison, Thank you for your review of our manuscript. Please consider the following responses to your concerns:

1 - As you mention, field logistics are challenging here, and for most of this research we did not have a profiling CTD at our avail. Anecdotally, we observe sediment laden plumes regularly boiling to the surface during energetic tides in all seasons, suggesting a physically well-mixed system. Shaha and Cho (2016) demonstrate minimal stratification in primary channel (Pussur) regardless of season, although they do indicate that early in the wet season (e.g., July) mixing between Shibsra and Pussur channels (which occurs in the Dhaki) can result in vertical stratification. Wilson et al. (AGU conference 2018) published observations of surface conductivity along a transect extending from the study area to the Bay of Bengal coastline in March 2015 (dry season). They demonstrate a consistent increase from P-32 (~24 mS/cm) to the coast of the Bay of Bengal (~40 mS/cm), supporting again that water columns are vertically mixed, rather than stratified.

We have included a figure with example ADCP cross-section velocity data, and SSC casts, to enhance transparency into our method.

2 – We will have added more detail to this calculation in the final version.

3 – Good point. We are well aware of the regional importance of tropical cyclones, and their potential to move sediment. We will update the text to include this discussion.

4 – Thank you for this clarification. In fact, the OBS deployed in the tidal channel was the same instrument used in the dry season field work (again – we were instrument-limited). The calibration was built from the >100 filtered water samples. We have restructured the methods to describe this calibration earlier on.

5 – Thank you. A similar concern was raised by Referee 1, and we invite you to consider our response to them.

1 **Observations and scaling of tidal mass transport across**
2 **the lower Ganges-Brahmaputra delta plain:**
3 **implications for delta management and sustainability**
4

5 Richard Hale¹, Rachel Bain², Steven Goodbred Jr.², Jim Best³

6 ¹Dept. of Ocean, Earth, and Atmos. Sci., Old Dominion University, Norfolk, VA, USA

7 ²Earth and Environmental Sciences Dept., Vanderbilt University, Nashville, TN USA

8 ³Departments of Geology, Geography & GIS, Mechanical Science and Engineering and Ven
9 Te Chow Hydrosystems Laboratory, University of Illinois, Urbana, IL USA

10
11 **Abstract**
12

13 The landscape of southwest Bangladesh, a region constructed primarily by fluvial
14 processes associated with the Ganges and Brahmaputra Rivers, is now maintained almost
15 exclusively by tidal processes as the fluvial system has migrated east and eliminated most
16 direct fluvial input. In natural areas such as the Sundarbans National Forest, year-round,
17 inundation during spring high tides delivers sufficient sediment that enables vertical
18 accretion to keep pace with relative sea-level rise. However, recent human modification of
19 the landscape in the form of embankment construction has terminated this pathway of
20 sediment delivery for much of the region, resulting in a startling elevation imbalance, with
21 inhabited areas often sitting >1 m below mean high water. Restoring this landscape, or
22 preventing land loss in the natural system, requires an understanding of how rates of water
23 and sediment flux vary across time scales ranging from hours to months. In this study, we
24 combine time-series observations of water level, salinity, and suspended sediment
25 concentration, with ship-based measurements of large tidal-channel hydrodynamics and
26 sediment transport. To capture the greatest possible range of variability, cross-channel
27 transects designed to encompass a 12.4-h tidal cycle were performed in both dry and wet
28 seasons, during spring and neap tides.
29

30 Regional suspended sediment concentration begins to increase in August, coincident with a
31 decrease in local salinity, indicating the arrival of the sediment-laden, freshwater plume of
32 the combined Ganges-Brahmaputra-Meghna rivers. We observe profound seasonality in
33 sediment transport, despite comparatively modest seasonal variability in the magnitude of
34 water discharge. These observations emphasize the importance of seasonal sediment
35 delivery from the mainstem rivers to this remote tidal region. On tidal time-scales, spring
36 tides transport an order of magnitude more sediment than neap tides in both the wet and
37 dry seasons. In aggregate, sediment transport is flood-oriented, likely a result of tidal
38 pumping. Finally, we note that rates of sediment and water discharge in the tidal channels
39 are of the same scale as the annually averaged values for the Ganges or Brahmaputra
40 rivers. These observations provide context for examining the relative importance of fluvial
41 and tidal processes in what has been defined as a quintessentially tidally influenced delta in
42 the classification scheme of Galloway (1975). These data also inform critical questions
43 regarding the timing and magnitude of sediment delivery to the region, which are
44 especially important in predicting, and preparing for, responses of the natural system to
45 ongoing environmental change.
46

Deleted: Champagne

Deleted: to the

Deleted: through the Holocene

Deleted: spring-tide

Deleted: for

Deleted: tidal

Deleted: somewhat

Deleted: ,

Deleted: indicating

Deleted: this

Deleted:

Deleted: the

Deleted: future change under

Deleted: changing

Deleted: conditions

62
63
64
65
66
67
68
69
70
71
72
73
74
75
76
77
78
79
80
81
82
83
84
85
86
87
88
89
90
91
92
93
94
95
96
97
98
99
100
101
102
103
104
105
106

1 - Introduction

The world's great deltas are currently threatened by a variety of factors, including global sea level rise (Overeem and Syvitski, 2009), overpopulation (Ericson et al., 2006), changes in sediment supply (Syvitski 2003; Syvitski and Milliman, 2007; Anthony et al., 2015; Darby et al., 2016; Best, 2019), and other human-related activities such as water diversions, flood control structures, and groundwater and hydrocarbon extraction (Syvitski et al., 2009). The Ganges-Brahmaputra-Meghna (GBM) delta is one of the most heavily populated regions that is undergoing locally accelerated sea-level rise (~0.5 cm/y; Higgins et al., 2014) due to a combination of natural and anthropogenic factors including eustatic sea-level change, tectonic subsidence, fine-grained sediment compaction, and groundwater extraction (Overeem and Syvitski, 2009; Syvitski, 2008; Steckler et al., 2010). In addition, when factors such as tidal amplification due to anthropogenic reworking of the distributary channel network are considered, the relative rate of sea-level rise can exceed 1.6 cm/yr (Pethick and Orford, 2013). Furthermore, the future viability of the delta is threatened by the proposed construction of dams and water diversions associated with India's National River Linking Project, which, if completed as proposed, could drastically reduce sediment delivery to Bangladesh (Higgins et al., 2018).

Restoration of land-surface elevation in many populated areas in the GBM delta is already necessary due to the relative loss in elevation that has occurred since the widespread construction of embankments during the 1960s to 1980s. Both planned (tidal river management) and unplanned (embankment failures) flooding of local polders (the embanked islands) has demonstrated the capacity of the natural system for effective sediment transport and deposition, with decimeters of annual accretion observed during recent breach events (Khadim et al., 2013; Auerbach et al., 2015; Kamal et al., 2017; Darby et al., 2018). One of the most important strategies that has been forwarded to reduce the threat of unintended inundations in SW Bangladesh is a plan for polder management (Brammer, 2014). However, many questions concerning potential management strategies remain, not the least of which are an accurate quantification of total available sediment mass and an understanding of the tidal processes involved in its transport and deposition. Toward these goals, the present study provides observation-based calculations of water and sediment transport through a major tidal channel in the delta across spring-neap tidal cycles and seasonal time scales, with the goal of identifying the timing and magnitude of mass sediment exchange between the different tidal channels. Not considered in the present study are the potential impacts of tropical cyclones, which directly impact Bangladesh 0.3-1.5 times per year (Murty et al., 2986; Alam et al., 2003; Saha and Khan, 2014), and can significantly affect the local landscape (Auerbach et al., 2015). The results presented herein are considered in the context of prior research concerning sediment accumulation and rates of channel infilling to better understand the role of tidal mass transport within the lower GBM delta plain.

2 - Background

Deleted: like

Deleted: the India

Deleted: rapidly and drastically

Deleted: These

Deleted: results

Deleted: then

113 Much of the low-lying coastal region of SW Bangladesh is under threat of long-term
114 inundation (Auerbach et al., 2015; Brown and Nicholls, 2015). The risk is particularly acute
115 for islands that were embanked (“poldered”) in the 1960s and 1970s as part of a program
116 designed to increase the area of arable land through the prevention of tidal inundation in
117 agricultural areas (Islam, 2006; Nowreen et al., 2014). Approximately 5000 km of polder
118 embankments were built by hand, generating 9000 km² of new farmland, but also
119 eliminating the semi-diurnal exchange of water and sediment between the tidal channels
120 and tidal platform (Islam, 2006; Nowreen et al., 2014). As a result, sediment resupply
121 pathways have been effectively terminated and the former floodplain surface in these
122 regions now lies 1.0-1.5 m below mean high water due to a combination of sediment
123 starvation, enhanced compaction, and tidal-range amplification (Auerbach et al., 2015;
124 Pethick and Orford, 2013).

Deleted: sediment

125
126 In contrast to the poldered landscape, the adjacent mangrove system of the Sundarbans
127 National Forest (SNF) is primarily inundated during spring high tides, and its
128 sedimentation and vegetation are keeping pace with sea-level rise (Rogers et al., 2013;
129 Auerbach et al., 2015). Protecting the SNF is of critical importance, as coastal wetlands and
130 mangroves provide irreplaceable ecosystem services including storm-surge buffering
131 (Uddin et al., 2013; Marois and Mitsch, 2015; Hossain et al., 2016; Sakib et al., 2015),
132 serving as effective carbon traps (McLeod et al., 2011; Alongi, 2012; Pendleton et al., 2012)
133 and perhaps even helping to combat the impacts of ocean acidification (Yan, 2016).
134

Deleted: ;

Deleted:

135
136 For the GBM delta, a unit-scale analysis of mass balance (Rogers et al., 2013) suggests that
137 the annual sediment load of the GBM river system (~1.1 Gt/y) is sufficient to aggrade the
138 entire delta system at rates ≥ 0.5 cm/yr, and thus provides potential to keep pace with
139 moderately high rates of sea-level rise. Such aggradation, of course, requires effective
140 dispersal of riverine sediment to disparate regions of the delta. Recent research suggests a
141 close coupling of discharge at the river mouth to sediment deposition in the remote delta
142 plain by way of tidal exchange (Allison and Kepple, 2001; Rogers et al., 2013; Auerbach et
143 al., 2015; Wilson et al., 2017). Such tidally supported sedimentation yields mean accretion
144 rates of ~1 cm/yr, with local observations regularly reaching 3-5 cm/yr, which together
145 indicate robust sediment delivery to the Sundarbans and SW coastal region (Rogers et al.,
146 2013; [Rogers and Overeem, 2017](#)). Thus, as the principal conduit for sediment that can
147 maintain the elevation of this region, an understanding and quantification of the tidal water
148 and sediment exchange is essential to foresee future impacts of accelerated sea-level rise
149 and the potential for mitigation.

Deleted:

150 3 – Methods

151 3.1 – Study Area

152 Our research concerns a network of tidal channels located approximately 80 km from the
153 coast along the Pussur River system, itself one of five similarly sized tidal distributary
154 networks (Fig. 1). Tidal exchange extends >120 km inland of the coast along the Pussur
155 River, with one branch ultimately connecting to the Gorai River, a distributary of the
156 mainstem Ganges River (Fig. 1). The tidal range along the Pussur River approaches its
157 maximum in the study area at 4-5 m for the spring tidal range, as compared with 3-3.5 m
158

163 on the coast at Hiron Point. The area is also societally relevant, lying at the transition from
164 the pristine Sundarbans forest to the embanked polders, and near the formerly active
165 shipping port of Mongla and cyclone- and flood- impacted island of Polder 32 (labelled P32
166 on Fig. 1; Auerbach et al., 2015).

167
168 Within this area, our observations were collected in the primary tidal channel of the Shibsra
169 River and two of its major bifurcations that connect with the Pussur channel, the Dhaki
170 River and Bhadra River (Fig. 1). The Shibsra River is the largest of these channels, with local
171 widths of 1-2 km, compared to 0.25-0.8 km and 0.15-0.3 km, for the Dhaki and Bhadra
172 Rivers, respectively. At its eastern extent, the Dhaki River connects to the Pussur River,
173 serving as the first major cross-channel to link the Shibsra and Pussur River channels after
174 they bifurcate ~60 km to the south (Fig. 1). At its upstream extent, the Pussur tidal channel
175 connects with the downstream mouth of the Gorai River, which delivers a water discharge
176 of ~3000 m³/s during the monsoon season and decreasing to ~0 m³/s during the dry
177 season (Winterwerp and Giardino, 2012). Salinity in the study area ranges from 0-1 PSU
178 during the monsoon, to 20-30 PSU during the dry season (Shaha and Cho, 2016; Ayers et
179 al., 2018). This seasonal variation in salinity is controlled by local runoff, freshwater
180 discharge from the Gorai River, and to a much larger extent, the magnitude of the regional
181 discharge plume of the GBM rivers (Rogers et al., 2013).

Deleted: the

182 183 3.2. - Hydrodynamic Observations

184
185 To establish tidal stage and capture surface-water elevations during the hydrodynamic
186 surveys, pressure sensors were deployed at multiple locations across the study area (Fig.
187 1). All sensors were deployed as close to low water as possible and recorded at 5- or 10-
188 minute intervals. Periods of subaerial sensor exposure (of up to 150 minutes at low tide)
189 were interpolated using a robust ordinary least-squares method provided by Grinsted
190 (2008). The agreement between measurement and prediction was generally good, with
191 predicted range being 0.98 of the measured range for a given time period, thus suggesting
192 that the interpolated data are both reasonable and conservative. The values reported
193 herein are of the interpolated values. Tidal range, water temperature, and conductivity
194 have also been monitored continuously since 2014 at the Sutarkhali station (Fig. 1B), with
195 an optical backscatter sensor (OBS) calibrated to measure suspended sediment
196 concentration (SSC) added in late March 2015. Prior to deployment in the tidal channel,
197 this OBS was used to measure vertical profiles of SSC on the Shibsra River, with
198 simultaneous water samples being collected to calibrate the instrument response to SSC.
199 Water samples were filtered using pre-weighed 0.4-µm nitrocellulose filters and washed
200 with freshwater to remove salts. The filters were then dried overnight and re-weighed to
201 determine the volume-concentration of sediment. The OBS measurements were calibrated
202 by comparing the voltage response observed in the field with the measured concentrations
203 from the same time and location, in a method modified from Ogston and Sternberg (1999).
204 Correlation between filtered samples and instrument voltage was strong, with an average
205 r-squared value of 0.83±0.1. While the sediment concentrations recorded by this near-bed
206 instrument are not directly comparable to the depth-averaged measurements made during
207 the present cross-channel surveys, we herein use these data to extend our understanding
208 of system behavior between the dry and monsoon seasons. For broader context, data from

210 the sensors deployed at the Sutarkhali station are also compared to monthly averaged
211 water discharge for the Ganges and Brahmaputra rivers for the period 1980-2000, based
212 on data from the Bangladesh Water Development Board, and Ganges River sediment
213 discharge data digitized from Lupker et al. (2011).

214
215 To quantify water and sediment flux in this area of the tidal transport system, cross-
216 channel hydrodynamic surveys were conducted during spring and neap tidal conditions at
217 two transects on the Shibsa River during the dry (March 2015) and wet
218 (August/September 2015) seasons. An additional wet season transect was also conducted
219 during moderate tides on the Pussur River. On the Shibsa River, the southern transect was
220 located south of the poldered landscape and entirely within the confines of the [Sundarbans](#)
221 [forest](#) (Fig.1). The northern transect was located ~12 km upstream in the poldered region,
222 just south of the Dhaki-Shibsa confluence and adjacent to Polder 32 to the east and Polder
223 10-12 to the west (Fig. 1B). Two secondary channels are present between these transect
224 locations that divert water onto the Sundarbans tidal platform and associated creek
225 network. Dry season surveys at both the southern and northern transects took place during
226 peak neap (15-16 Mar) and spring (21-22 Mar) tides. During the ensuing monsoon season,
227 spring tides were measured on August 30-31 (southern transect) and September 2
228 (northern transect), followed by neap tides on September 7 and 8 (northern and southern
229 transects, respectively). Surveys lasted for 11-13 hours as conditions allowed,
230 encompassing approximately one-half of a tidal cycle (i.e., one high and one low tide).
231 Because this system is largely semi-diurnal with a minimal mixed component, we are
232 confident that this time interval was long enough to [accurately](#) describe the system
233 dynamics.

234
235 The surveys were conducted using Sontek M9 multi-frequency ADCPs to collect flow-
236 perpendicular observations of current velocity and direction. Data were collected at 1 Hz,
237 using both 1.0 and 3.0 MHz transducers, resulting in vertical bins ranging in height from
238 0.1-1.0 m. From these values, total discharge was calculated by integrating velocity over
239 space and time. River conventions are used for presenting velocity and discharge data,
240 where positive values refer to the ebb or downstream direction and negative values for the
241 flood or upstream transport. A typical survey day included 50-60 individual river crossings
242 at the transect location, measuring cumulative discharge in both directions across the
243 channel. [Examples of cross-channel transects of velocity and SSC used to compute](#)
244 [instantaneous water and sediment discharge can be found in Figure 2.](#) Because surveys
245 could only be conducted during daylight hours and as weather conditions allowed,
246 discharge is interpolated to complete a 12.4-hour tidal cycle, which is the average tidal
247 cycle duration in the area (range: 11.9-13.1 h). By assuming that the change in tidal prism
248 is negligible between consecutive tides, as suggested by the similarity in tidal elevations
249 ([Fig. 3](#)), we can tile measurements in 12.4 h increments and interpolate using a cubic
250 spline. Working conditions were particularly challenging during the monsoon season,
251 resulting in especially short-duration survey days. In the absence of measured discharge,
252 we use a mass balance approach to constrain the magnitude of the missing tidal prism data.
253 For the monsoon-season spring tides, we treat the region between the southern and
254 northern transects and the southern Bhadra River as a closed system with no long-term
255 (>1 semidiurnal period) water storage. Using measured Bhadra River discharge values and

Deleted: SNF

Deleted: accurately

Deleted: '

Deleted:

Deleted: Fig. 2

261 assuming a negligible to slightly southerly-directed net flux through the adjacent
262 Sundarbans, allows us to determine the likely range of values for the unmeasured ebb
263 prism at the southern transect. For the monsoon-season neap tides, we consider the larger
264 region bounded by the southern transect to the southwest, the Pussur River below the
265 Dhaki River confluence to the southwest, and the Bangladesh Water Development Board
266 gauging station at the Gorai Railway Bridge ~275 river km to the north. Balancing the
267 measured net flux through the Pussur River and the recorded upstream discharge of the
268 Gorai River of 3000 m³/s with the measured ebb prism at the southern transect allows us
269 to estimate the missing southern transect flood prism. We then repeated this spring tide
270 procedure to estimate the unmeasured neap flood prism at the northern transect.

272 3.3 – Sediment Observations

274 In addition to water discharge, observations of SSC along the transect lines were made
275 using a combination of filtered water samples and optical-backscatter (OBS)
276 measurements. While the exact sampling method varied depending on available
277 instrumentation and river conditions, the general approach involved collecting OBS
278 profiles to the maximum possible depth (<10 m), at either two (northern transect) or three
279 (southern transect) locations along the channel edges and centerline (Figs 1, 2). OBS
280 measurements were supplemented by simultaneous water samples (100-200 ml) collected
281 from various depths using a Niskin sampler, which were used to calibrate the OBS as
282 described above (Section 3.1).

284 In order to calculate total sediment fluxes, the vertically and horizontally distributed SSC
285 observations collected for each channel cross-section were averaged to produce a series of
286 temporally discrete SSC values over the course of one tidal cycle (Figs 2, 4). This spatial
287 averaging appears suitable because the variance was considerably smaller than the
288 temporal variability associated with tidal discharge and strong seasonal contrasts. Using
289 wet season data as an example, the average standard deviation of SSC through time at one
290 sample location was 0.2 g/L, while the average standard deviation of SSC between stations
291 at any given time was 0.13 g/L. When conditions did not allow samples to be collected at
292 depths below the water surface, a scaling factor of 1.25 was applied to account for the
293 higher sub-surface SSC, which we determined by the relationship between depth-averaged
294 concentrations and surface concentrations from the other available data. Similarly,
295 measurements from 15 March (dry-season neap tide) were only collected at depths of 5
296 and 15 m and were thus scaled by a factor of 0.81 to be comparable to other measurements
297 that included surface SSC values.

299 An important caveat for all SSC measurements is that we present data collected primarily
300 from the upper water column and not sampled isokinetically, due to instrument limitations
301 and high current velocities. Thus, our values principally represent suspended load and do
302 not account for bedload transport, which likely represents an additional component of total
303 sediment transport. As with our water-discharge measurements, SSC values were
304 calculated over an entire tidal cycle by repeating a measured time series in 12.4-hour
305 increments, then interpolating using a cubic spline. From these values, the integrated

Deleted: Fig.

Deleted: . Water samples were filtered using pre-weighed 0.4- μ m nitrocellulose filters and washed with freshwater to remove salts. The filters were then dried overnight and re-weighed to determine the volume-concentration of sediment. The OBS measurements were calibrated by comparing the voltage response observed in the field with the measured concentrations from the same time and location, in a method modified from Ogston and Sternberg (1999). Correlation between filtered samples and instrument voltage was strong, with an average r-squared value of 0.83 \pm 0.1.

Deleted: the

Deleted: because

Deleted: are dealing mostly

Deleted: with

Deleted: and

Deleted: ing

Deleted: ,

Deleted: what we are referring primarily to measuring

Deleted: is primarily

Deleted: or fine flux,

Deleted: we

Deleted: are largely ignoring the

Deleted: component

Deleted: . While this

Deleted: is presumably a measurable

Deleted: the

Deleted: ,

Deleted: bedload is likely unable to exit the tidal channels during platform irrigation

Deleted: challenging field conditions preclude our ability to directly measure it, and as such is not considered an important source of sediment for land construction. ...

Deleted: of water discharge

Deleted: tiling observations

Deleted: segments

Deleted: and

345 product of water discharge and SSC yields net sediment flux, which we compute using the
346 time series for each component as calculated using the aforementioned methods.

347
348

349 4 – Results

350

351 4.1 – Long-term Pressure and OBS

352

353 At our long-term station deployed in a secondary tidal channel (Fig. 1), recorded water-
354 level variations show tidal-period excursions with a range of 1.8 to 4.8 m over the 12
355 months of observation (Fig. 3). This variance is, of course, driven primarily by the
356 fortnightly spring-neap tidal cycle, but there is also a seasonal variability showing the
357 monsoon period to have a reduced tidal range as compared with the dry season. In this
358 case, the neap tidal range is ~10% less during the monsoon season, and the spring tidal
359 range is as much ~20% less, accounting for a nearly 1 m difference (3.9 m vs. 4.8 m). This
360 reduced range in the monsoon season, however, is not manifested in the elevation of high-
361 tide water levels, which remained largely consistent between seasons. Rather, the
362 difference is caused by higher water levels during low tide (Fig. 3), which has the effect of
363 truncating the tidal range and yielding an overall higher mean water level. These higher
364 low-water levels associated with the monsoon suggest that they are tied to regional
365 freshwater drainage and discharge. In addition, another contributing factor could be the
366 seasonally reversing monsoon wind stresses, but such set-up should enhance high water
367 levels as well, suggesting that they are not the primary cause. Although further research on
368 this topic is needed, these distinctions are important herein for understanding the behavior
369 of the tidal delta plain, as landscape elevations in this region are closely tied to mean high-
370 tide water levels, and not mean sea level (Auerbach et al., 2015). Thus, as first
371 demonstrated by Pethick and Orford (2013), the monthly mean tide-gauge data often used
372 to track seasonal to interannual variations in water level may have relatively little bearing
373 on the tidal inundation period and sedimentation rates that control tidal platform elevation
374 (Rogers et al. 2013).

375

376 The arrival of fully fresh water (wet-season) conditions occurs in July, following the peak in
377 Brahmaputra River water discharge, and roughly coincident with peak Ganges River water
378 discharge (Fig. 4). Coupled with our long-term pressure gauge, the OBS sensor recorded
379 relatively constant, but low, mean SSC from the late dry season into the early monsoon
380 period (late March through July), with weak but noticeable spring-neap variability ranging
381 from ~0.01 g/L to 0.20 g/L (Fig. 3). However, moving into peak monsoon season, SSC
382 increases markedly from early August through September, concurrent with the Ganges
383 River sediment discharge peak (Figs 2, 3). Individual measurements regularly exceeded
384 0.50 g/L during this time, with maxima >2.5 g/L (Fig. 3). SSC variability around the semi-
385 diurnal tide and spring-neap cycles was greatly enhanced compared with that during the
386 dry season, with SSC values during spring tidal cycles exceeding those observed during
387 neap conditions by a factor of 2-10. By the end of observations in October 2015, SSC began
388 to drop to levels similar to those observed in mid-August (0.01-1.0 g/L; Fig. 3), but on
389 average remained well above those of the dry season. For comparison, the mean annual
390 SSC of the mainstem Ganges-Brahmaputra river is ~1 g/L, and depth-averaged values in

Deleted :

Deleted: Fig. 2

Deleted: Fig. 2

Deleted: Fig. 3

Deleted: Fig. 2

Deleted: Figs.

Deleted: Fig. 2

Deleted: Fig. 2

399 the main estuary mouth and on the inner shelf commonly range 2-5 g/L during high river
400 discharge (Barua et al., 1994; Ali et al., 2013). In total, SSC values well in excess of 1 g/L are
401 regularly observed during the wet season from the mainstem river to the inner shelf and
402 into the tidal channels of the lower delta plain. These results support previous evidence for
403 the strong coupling of seasonal river discharge with penecontemporaneous sedimentation
404 in the remote tidal delta plain (Rogers et al., 2013).

406 4.2 – Hydrography – Water Discharge,

407
408 Dry season tidal range on the Shibsa River, as measured at Nalian near the northern
409 transect (Fig. 1B), varied from 2.3 m during the neap minima to 5.6 m during spring
410 maxima (Fig. 3). The tidal period was slightly longer during neap tides than spring tides
411 (12.9 h vs. 12.3 h), and the mixed component of the semi-diurnal tide was more
412 pronounced, with consecutive tidal ranges varying by as much as 0.55 m during neap tides,
413 versus 0.23 m during spring tides (Fig. 3). During the monsoon fieldwork, the tidal range
414 was 2.4 and 4.2 m for neap and spring tides, respectively. As with the dry season, total tidal
415 period during neap tides was slightly longer than spring tides (12.8 h vs. 12.0 h). The mixed
416 semi-diurnal variability was again greater during neap tides as well, which varied by as
417 much as 0.25 m, while spring tide variability was typically <0.10 m (Fig. 3).

418 In this study, we calculate the tidal prism by integrating water discharge over the
419 individual ebb and flood limbs of the tide, with net discharge calculated as the difference
420 between them. During the dry season, our observations captured both peak flood and ebb
421 discharges, with interpolation being used over the remaining <5-15% of the tidal cycle (Fig.
422 5). During the wet season, field conditions during several surveys limited our measurement
423 to only a partial tidal cycle (~8-9 hr survey; Fig. 5). Only during northern transect spring
424 tides were conditions favorable for collecting observations of similar duration to the dry
425 season (~11 hr survey; Fig. 5). Within these limits, however, we have used conservative
426 interpolation methods to generate error-bound estimates of total water discharge, the
427 resulting patterns of which provide robust observations concerning system behavior (see
428 Section 2; Fig. 5).

430
431 The average tidal-prism magnitudes for the northern and southern transects are $2.1 \pm 0.7 \times$
432 10^8 m^3 and $3.4 \pm 1.4 \times 10^8 \text{ m}^3$, respectively. Included in these averages are the absolute
433 values of flood and ebb tidal prisms measured on spring and neap tides during both wet
434 and dry seasons (Table 1). Thus, the tidal prism at the northern transect averages only
435 ~60±10% that of the southern transect regardless of season, even though they are located
436 just 10 km apart. Most of this difference in discharge (c. 80-100%) can be balanced by
437 water storage between the two locations, where the product of tidal range and area
438 between transects is c. $6.7 \times 10^7 \text{ m}^3$. Considering differences in seasonal discharge, results
439 show that the neap ebb prism is ~30% greater during the monsoon at both transects,
440 despite having a smaller tidal range compared with the dry season survey. This difference
441 of $4-6 \times 10^7 \text{ m}^3$ equates to an excess ebb discharge of 1800-2800 m^3/s , which is about 45-
442 70% of the mean monsoon discharge of the upstream Gorai River. We thus take the greater

Deleted: :

Deleted: Fig. 2

Deleted: Fig. 2

Deleted: the

Deleted: Fig. 2

Deleted: In order to

Deleted: dry-season

Deleted: the

Deleted: (i.e., integrated

Deleted: discharges

Deleted: t

Deleted:)

Deleted: Fig. 4

Deleted: monsoon

Deleted: challenging

Deleted: resulted in

Deleted: capturing

Deleted: Fig. 4

Deleted: Fig. 4

Deleted: Fig. 4

Deleted: tidal

Deleted: river

465 wet-season ebb prism to simply reflect the addition of local freshwater discharge from the
466 Gorai River (Table 1; Fig. 1).

467
468 Strictly speaking, defining a tidal regime as either ebb- or flood- dominant refers to the
469 water velocity rather than discharge (Pethick, 1980; Brown and Davies, 2010). In the
470 present study, however, we are interested in the net movement of water and sediment and
471 thus refer to a particular discharge regime as either ebb or flood “dominated” or “oriented”
472 based on the net tidal prism (i.e., the difference between ebb and flood discharge). With
473 this in mind, our surveys suggest that the system varies between ebb and flood orientation
474 across both tidal phase and season (Table 1). For example, both transects during the dry,
475 spring and wet, neap surveys show the average ebb-tidal prism to be $26 \pm 16\%$ larger than
476 the flood limb. In contrast, the other two survey periods (dry, neap and wet, spring)
477 yielded balanced to slightly flood dominated tidal prisms ($9 \pm 8\%$). In summary, although
478 our results on water balance are insufficient for a full understanding of the patterns, a key
479 finding is that the ebb and flood tidal prisms rarely balance at this location. These tidal-
480 prism asymmetries appear to be a salient characteristic of the complex, interconnected
481 channel network of the GBMD tidal delta plain. Thus, even our limited observations require
482 a lateral (east-west) exchange of water between the Shibsa and parallel Pussur channels
483 (Fig. 1), which we presume to be driven by locally non-uniform tidal phasing within the
484 channel network. Given these emergent circulation patterns, it is clear that individual
485 channels do not operate as closed systems and exhibit local, non-uniform mass exchange,
486 providing a first indication of how morphologic evolution of [this tidal delta plain and its](#)
487 [channel network may](#) occur,

488
489 Although [relative dominance between the ebb and flood tidal prisms](#) [persistently](#) covaries
490 [\(as described above\)](#), the mean and instantaneous water discharge (m^3/s) is almost always
491 flood-dominant (Fig. 6). This circumstance arises from the significant phase shift that
492 occurs as the tide wave propagates up channel, resulting in a shorter flood period and thus
493 higher peak discharge. From our measurements of instantaneous discharge across seasons
494 and tidal conditions, we calculate mean ebb and flood discharges (m^3/s) for each transect
495 (Fig. 6). Mean discharge for the northern transect is $\sim 9100 \text{ m}^3/\text{s}$ on the flood and 8600
496 m^3/s on the ebb, and for the southern transect, mean flood and ebb discharges are $\sim 14,600$
497 and $14,200 \text{ m}^3/\text{s}$, respectively. From these results, we observe that mean discharge at the
498 northern transect is again $\sim 61 \pm 1\%$ that of the southern transect, as also recognized for the
499 tidal prism. Another notable result is that the mean flood discharge (m^3/s) is 3-6% greater
500 than on the ebb tide, despite the tidal prism generally being ebb dominant. This disparity is
501 a function of the shallow-water distortion of the M2 tide, which produces an asymmetrical
502 waveform with a steeper rising limb than falling limb, and a corresponding reduction in the
503 duration of the flood tide by $\sim 60-90$ minutes.

504 505 506 **4.3 – Hydrography – Sediment Transport**

507
508 Suspended sediment measurements collected during the hydrographic surveys show
509 similar patterns to those of our long-term OBS station. Wet season sediment concentrations
510 were generally 30-50% higher than during the dry season (Fig. 5). Much greater

Deleted: the

Deleted: s

Deleted: the

Deleted: persistently

Deleted: Fig. 5

Deleted: Fig. 5

Deleted:

Deleted: ing

Deleted: :

Deleted: Fig. 4

521 differences in SSC were observed, however, between neap and spring tidal conditions, with
522 the latter concentrations being typically ~3 fold greater (0.3-1.5 g/L vs 0.1-0.5 g/L). These
523 sediment concentrations, coupled with the water discharge observations, were then
524 extrapolated over the tidal cycle to generate estimates of the rates and magnitude of
525 sediment transport (Table 1). Results show that integrated sediment transport over a tidal
526 limb varied by more than an order of magnitude at both transects. Minima of 0.16×10^8 kg
527 (north) and 0.2×10^8 kg (south) of sediment exchange were observed during the neap, dry-
528 season ebb tide, with maxima during spring, monsoon flood tides being an order of
529 magnitude greater at 3.3×10^8 kg (north) and 3.9×10^8 kg (south). These values equate to
530 mean rates of sediment transport ranging from ~700 kg/s during neap, dry season
531 conditions to ~17,000 kg/s during monsoon-season spring tides. Comparing the ebb and
532 flood limbs of our surveys, the mean sediment discharge for the ebb tide is 5800 kg/s
533 compared to 7800 kg/s for the flood tide, demonstrating an overall flood dominance in
534 sediment transport.

535
536 These patterns are further supported by the net sediment transport values (i.e., ebb – flood;
537 Table 1). For a given tidal cycle, net sediment transport was typically 10^6 - 10^7 kg, with
538 magnitude varying largely with tidal phase, where spring tides generate 1.5 to 3 times
539 greater net transport than during neap tides (Table 1). Seasonally, net sediment transport
540 rates were ~30% greater during the wet season, similar to our observations of suspended
541 sediment concentration. Finally, a comparison of net sediment transport with
542 corresponding net water discharge shows the two to covary, as expected, with greater net
543 water discharge resulting in greater net sediment transport (Fig. 7). However, an important
544 attribute of this relationship reveals a significant bias toward flood-dominant sediment
545 transport. Data show that even neutral to weakly ebb dominant water discharge yields net
546 sediment transport in the flood direction (Fig. 7). As noted for water discharge (m^3/s), this
547 disparity is a function of the non-negligible tidal components beyond M2 that result in a
548 shortened flood limb and extended ebb period (Fig. 3; Table 1). Together, mean sediment
549 discharge and net sediment transport patterns thus indicate an overall flood-oriented
550 asymmetry and net onshore transport of sediment.

551 552 553 **5 - Discussion**

554 555 **5.1 – Relative importance of tides and river**

556
557 The GBM tidal delta plain comprises a complex channel network that has been little studied
558 and will require substantial investigation to be understood well. Nevertheless, results of
559 the current study allow for numerous observations on the scaling and magnitude of tidal
560 mass transport within this region, establishing a baseline for the role that tides play in
561 defining the delta system, particularly in the southwest region away from direct fluvial
562 inputs. To begin, we take an average of the flood and ebb tidal prisms measured at the two
563 sites on the Shibsra River over both spring and neap tidal phases during wet and dry
564 seasons, and extrapolate the mean tidal prism over one year. In other words, an average of
565 $2.7 \times 10^8 m^3$ water passes through this region on each of the ~705 tides per year. This basic

Deleted: and

Deleted: of

Deleted: occurred on the spring, monsoon flood tides

Deleted: that range

Deleted: Fig. 6

Deleted: Fig. 6

Deleted: Fig. 2

573 estimation accounts for an average of $\sim 2 \times 10^{11}$ m³ of water annually conveyed through
574 our survey locations, 80 km inland of the coast. Furthermore, this mass exchange is
575 principally tidal water, as the 50-75% of annual Gorai River discharge captured by the
576 Shibsra River (i.e., $\sim 0.2 \times 10^{11}$ m³) accounts for only 10% of the total water exchange
577 observed for that channel.

578 The significance of these observations from the upstream Shibsra River tidal channel
579 become more apparent when compared with the mainstem GBM rivers. In this case, the ~ 2
580 $\times 10^{11}$ m³ of water conveyed annually through the upper Shibsra River is nearly 20% of the
581 $\sim 11 \times 10^{11}$ m³ of total annual water discharge from the entire GBM watershed (Lupker et
582 al., 2011; Fig. 4). This is an impressive exchange of mass through the upper reaches of a
583 single tidal channel along the GBM tidal delta plain. For context, the Shibsra River
584 comprises approximately half (by planform area) of the Pussur River tidal system (Fig. 1),
585 itself just one of five major tidal drainages along the GBM tidal delta plain (Fig. 1). Taken
586 together, these basins include ~ 10 tidal channels having similar area (width \times length) to
587 the Shibsra River. We take the tidal flow through these systems to be broadly similar given
588 the linear relationship between peak tidal discharge and the cross-sectional area of large
589 tidal channels (Rinaldo et al., 1999), plus the fact that land-surface elevation and tidal range
590 are similar across the region (Chatterjee et al., 2013). Thus, even at a first-order, estimates
591 of total mass transport across the tidal region would well exceed the $\sim 11 \times 10^{11}$ m³ total
592 volume discharged by the mainstem GBM rivers.
593

594 The comparable values between our observations of tidal water exchange in this limited
595 study area and the total freshwater discharge of the GBM rivers demonstrates how tides
596 hold equivalence in controlling landscape development in the GBMD, which was suggested
597 as far back as Galloway (1975). To further consider the geomorphic importance of tides to
598 the GBMD, we make analogous estimations of the sediment transport (Q_s) that supports
599 land-surface aggradation and the dominant water discharge (Q_{dom}) that controls tidal
600 channel morphology (Rinaldo et al., 1999). As done for water discharge, by taking the
601 average of our tidal hydrography data for sediment transport, we calculate a mean annual
602 exchange of suspended sediment through the Shibsra River tidal station to be $\sim 1 \times 10^{11}$ kg
603 (~ 100 Mt). For comparison, this estimate of sediment load is roughly 15% of the ~ 700 Mt
604 of sediment annually discharged to the coast by the GBM rivers (Goodbred and Kuehl,
605 1999). Thus, if we extrapolate any similar transport value to the other nine GBM tidal
606 channels, then the sediment exchange through the tidal channels is easily found to be
607 comparable to the main river mouth. There is, of course, the important caveat that tidal
608 sediment transport is not unidirectional, and so this integrated exchange of tidal sediment
609 is not a net flux as it is for river sediment discharge. Nevertheless, the relevant point is that
610 local, geomorphic reaches of the tidal delta plain have the opportunity for landscape
611 building through tidal water and sediment exchange at a similar magnitude to the
612 mainstem GBM rivers. This assertion is not surprising given the relative stability of the
613 tidal delta plain, which experiences relatively little net erosion (~ 4 km²/yr, or $\sim 0.02\%$
614 annual loss; Sarwar and Woodroffe, 2013) and is offset by widespread sediment deposition
615 on both land-surface (Rogers et al., 2013) and in channels (Wilson et al., 2017).
616
617

Deleted: Fig. 3

Deleted: GMB

Deleted: This

Deleted: magnitude

Deleted: of

Deleted: the

Deleted: comparable

Deleted: importance

Deleted: further

Deleted: very

Deleted: ,

Deleted: the

630 From this study, we understand that tidal energy, independent of the main river mouth,
631 accounts for a twice-daily exchange of a mass equivalent to 4-15% of the yearly averaged
632 daily GBM river discharge. In primary channels, the magnitude of this exchange is
633 controlled more by the spring-neap tidal variability than by the seasonal input of new
634 material (Fig. 5). In the smaller Bhadra tidal channel, on the other hand, SSC variability
635 demonstrates profound seasonality, presumably because discharge (and therefore stream
636 power) is at least an order of magnitude smaller here than in the Shibs River. This
637 disparity is important when we consider land-building processes, as the majority of the
638 Sundarbans forest is plumbed by tidal channels on the scale of the Bhadra River or smaller.
639 Storms may also play a role in remobilizing sediment from the shelf onto the tidal
640 delta plain, as suggested by Hanebuth et al. (2013) in their study of ancient salt kilns buried
641 along the coast. However, there are no observations of significant direct storm deposition
642 from recent cyclones (Aila, 2009 and Sidr, 2007), such as that recognized from the offshore
643 Bengal shelf and Swatch-of-No-Ground canyon (e.g. Kudrass et al., 1998; 2018; Michels et
644 al., 1998; Rogers et al., 2015). The potentially limited impact of storms on sedimentation
645 and the channel network of the tidal delta plain may be due its frequent and persistent
646 exposure to high sediment concentrations and strong currents (>3 m/s) driven by the
647 tides. Nevertheless, future research should aim to quantify storm inputs and their relative
648 importance upon sedimentation and morphodynamics of the tidal delta plain.

650 These findings and discussion points emphasize the essential role that tides play in
651 maintaining the largest portion of the GBM lower delta plain, which is not under direct
652 river influence. However, despite the essential role of tides in mixing and dispersing
653 sediment to large areas of the delta, the supply of sediment remains largely
654 contemporaneous with seasonal fluvial discharge, especially in the secondary and tertiary
655 channels that irrigate the Sundarbans. Together, the coupled system in which the GBM
656 rivers deliver sediment that is subsequently redistributed by tidal energy is fundamentally
657 responsible for sustainability of this region relative to sea-level change (e.g., Angamuthu et
658 al., 2018). A significant corollary of this fact is that a change in sediment supply from the
659 GBM rivers, such as that proposed under India's National River Linking Project, could pose
660 a serious threat to delta sustainability (Higgins et al., 2018; Best, 2019).

662 To summarize, as the central coastal region receives little direct water and sediment
663 discharge from the GBM, the results herein emphasize that tidal exchange is the dominant
664 geomorphic agent in the region with a mass and energy exchange of comparable or greater
665 magnitude to the mainstem rivers. It is, of course, essential to recognize that most
666 freshwater and sediment exchanged within the tidal system is ultimately sourced by the
667 main rivers, and that these are intrinsically coupled systems. Thus, continued sustainability
668 of the region will require the sustained delivery and exchange of water and sediment
669 between the fluvial and tidal portions of the delta.

671 5.2 – Sedimentation in the Sundarbans and Infilling of Tidal Channels

673 Our observations of tidal sediment exchange provide a useful baseline for examining
674 sedimentation in the Sundarbans and broader tidal delta plain, which are at risk from sea-
675 level rise and inundation without an adequate supply of sediment. To date, the best

Deleted: rather

Deleted: Fig. 4

Deleted: BR

Deleted: SNF

Deleted: BR

Deleted:

Deleted:

Deleted:

Deleted: the

Deleted: to

Deleted: dispersal

Deleted: almost wholly derived from the river mouth
and ...

Deleted: SNF

Deleted: the

691 estimate of total sedimentation in the Sundarbans is 1.1×10^{11} kg/year (~100 Mt), based
692 on one season of direct sedimentation measures at 48 stations across the region (Rogers et
693 al., 2013). This mass of sediment deposited in the Sundarbans is basically equivalent to the
694 ~100 Mt of sediment that we observe transported through the Shibsra River transects.
695 Thus, recalling that our local measurements likely capture just 5-10% of total suspended
696 sediment transported through the tidal channels of the region, it becomes evident that
697 there is generally adequate suspended sediment available to support regional
698 sedimentation in the Sundarbans.

700 Another plausible implication is that there appears to be adequate sediment available for
701 the restoration of land elevation within the poldered region, which is a major challenge
702 facing coastal Bangladesh (Amir et al., 2013). Although a definitive answer remains to be
703 determined, this general assertion is supported by observations of the rapid sedimentation
704 that occurred on Polder 32 in the two years following the embankment failures caused by
705 cyclone Aila in 2009 (Auerbach et al., 2015). Measurements at Polder 32 after these
706 failures found an average of 37 ± 17 cm/yr of tidal sedimentation sustained over its two-
707 year exposure to tidal inundation, corresponding to a total annual deposition of ~5 Mt.
708 Based on inundation depth and period, this accounts for an average of ~0.2 g/L of sediment
709 extracted from the tidal waters that flooded the island during this time. This value
710 compares to a mean suspended sediment concentration of ~0.6 g/L measured during our
711 hydrographic surveys, suggesting that roughly one-third of the tidal sediment inundating
712 the landscape generated these very rapid sedimentation rates. Ultimately, limitations in the
713 present data preclude a closed, precise sediment budget, but our collective observations
714 over several different studies remain consistent in direction and magnitude. These indicate
715 persistent, relatively rapid, rates of deposition that are sustained by the large-magnitude
716 conveyance of sediment through the tidal channels and ultimately supplied by seasonal
717 discharge of the mainstem rivers (Rogers et al., 2013; Auerbach et al., 2015; this study).

719 Upstream of our transect sites, the landscape is almost entirely embanked by polder
720 systems. With limited opportunity for sediment deposition on this formerly intertidal
721 platform, and with the resulting reduction or redistribution of the tidal prism upstream,
722 channel sedimentation and infilling has become a major problem. Wilson et al. (2017)
723 demonstrate that by preventing the inundation of the intertidal platform, poldering has
724 reduced the tidal prism of the broader southwest region by as much as 1.4×10^9 m³. If we
725 assume that this volume reduction is relatively evenly dispersed across the delta plain,
726 then it would have led to a 25-50% reduction in the local tidal prism measured at our sites.
727 These effects are at least partially responsible for the ~1400 km of channel infilling that
728 has taken place over the last few decades, resulting in the creation of new agriculture and
729 aquaculture opportunities but also altering drainage, transportation routes, and feedback
730 responses of the regional tidal hydrodynamics (Wilson et al., 2017). The mass of sediment
731 that has infilled these channels is calculated to be 6.15×10^{11} kg, which would be $\sim 1.2 \times$
732 10^{10} kg/yr assuming a roughly constant rate (Wilson et al., 2017). Of these infilled
733 channels, ~15% (~200 km) are part of the former channel network connecting upstream
734 of our northern transect (Fig. 1). Thus, a proportional rate of sedimentation lost to these
735 channels would be $\sim 0.18 \times 10^{10}$ kg/yr, which is ~25% of the estimated 0.68×10^{10} kg

Deleted: during

Deleted: a

Deleted: period

Deleted: for

Deleted: in

741 fluxing through the northern transect (to the north) each year. While this sediment
742 [exchange](#) is four times greater than the expected total based on infilling rates from Wilson
743 et al. (2017), it relies on the same previously described assumptions (i.e., no lateral
744 exchange with neighboring rivers, non-end-member flux reflecting an average of end-
745 member conditions). More importantly, it appears that there is sufficient sediment
746 available to continue infilling channels, and future studies should constrain whether this
747 region is, in fact, infilling faster than other areas on the tidal delta plain, as this would hold
748 important implications for regional navigation and hydrodynamic changes.

Deleted: flux

750 6 – Conclusions

751
752 In the present study, we have measured tidal and seasonal variability associated with
753 water discharge and suspended sediment concentration (SSC), and used these observations
754 to compute the magnitude of water and sediment exchange through a single tidal channel.
755 As has been suggested previously, the wet season is found to exert a strong control on the
756 timing and magnitude of sediment transport in this system, despite seemingly modest
757 changes to the hydrodynamics. Indeed, despite a reduced tidal range and similar peak SSC,
758 sediment transport during the monsoon is always of greater magnitude than during the dry
759 season. Understanding this relationship is critical for planning any potential land recovery
760 strategies in the future. The importance of the monsoon also provides a new perspective
761 into the meaning of a “tidal delta.” While it is clearly the tides that perform much of the
762 work to shape the delta – including driving a net flood-oriented direction of sediment flux –
763 it is the seasonal influx of riverine sediment that allows this work to continue. Finally, this
764 research demonstrates that the mass of sediment transported north of our study area is
765 more than sufficient to fill channels and create additional land. Ideally, future land-use
766 management strategies [could](#) divert some of this excess sediment into polder interiors
767 through tidal river management ([e.g., Seijger et al., 2018; Shampa et al., 2012; van Staveren](#)
768 [et al., 2016](#)), and allow this landscape to continue to prosper.

Deleted: should

770 Code availability:

771

772 Data availability:

773 Data used for this publication will be archived in the Marine Geoscience Data System.

774

775 Sample availability:

776 Samples from this publication are stored in the sedimentology laboratory at Vanderbilt
777 University

778

779 Author Contribution:

780 The experiment was designed by RH and SG, with input from RB and JB. RH and RB led the
781 field research efforts with support from SG and JB. RH wrote the majority of the manuscript
782 and figures, with substantial input from SG. RB and JB also contributed to the manuscript
783 and figures.

Deleted: a

785 Competing interests:

786 The authors declare that they have no conflict of interest.

790
791
792
793
794
795
796
797
798
799
800
801
802
803
804

Acknowledgements:

This work would not be possible without the support of our local collaborators, Drs. Kazi Matin Ahmed and Syed Humayun Akchter from Dhaka University, who oversaw in-country logistics and offer local guidance. We would also like to thank Abu Naser Hossain of the Forestry Crime Department for his help with permitting, and Nasrul Islam Bachchu of Pugmark Tours, and the captain and crew of the M/V Bawali and M/L Mawali for their seemingly endless patience with our field logistics. We would also like to thank Md. Saddam Hossain, Abrar Hossain, Mynul Hassan, Carol Wilson, and Mike Reed for their field support. This research was supported by the US Office of Naval Research (N00014-11-1-0683) and the National Science Foundation (Coastal SEES- #1600319).

Deleted: .
Deleted: oversee

807 **References:**

- 808
809 [Alam, M.A., Hossain, M.A., and Shafee S. Frequency of Bay of Bengal cyclonic storms and](#)
810 [depressions crossing different coastal zones. *International Journal of Climatology*, 23,](#)
811 [pp. 1119-1125, 2003.](#)
- 812 Ali, A., Mynett, A.E. and Azam, M.H. Sediment dynamics in the Meghna estuary, Bangladesh:
813 A model study. *Journal of Waterway Port Coastal and Ocean Engineering-ASCE*, 133:
814 255-263, 2007.
- 815 Allison, M. and Kepple, E. Modern sediment supply to the lower delta plain of the Ganges-
816 Brahmaputra River in Bangladesh. *Geo-Marine Letters*, 21(2), pp.66-74, 2001.
- 817 Alongi, D.M. Carbon cycling and storage in mangrove forests. *Annual Review of Marine*
818 *Science*, 6, pp.195-219, 2014.
- 819 Amir, M.S.I.I., Khan, M.S.A., Khan, M.K., Rasul, M.G. and Akram, F. Tidal river sediment
820 management-A case study in southwestern Bangladesh. *International Journal of*
821 *Environmental, Chemical, Ecological, Geological and Geophysical Engineering*, 7(3),
822 pp.176-185, 2013.
- 823 [Angamuthu, B., Darby, S.E., and Nicholls, R.J. Impacts of natural and human drivers on the](#)
824 [multi-decadal morphological evolution of tidally-influenced deltas. *Proceedings of the*](#)
825 [*Royal Society A*, 474, 20180396, 2018.](#)
- 826 Anthony, E.J., Brunier, G., Besset, M., Goichot, M., Dussoillez, P. and Nguyen, V.L. Linking
827 rapid erosion of the Mekong River delta to human activities. *Scientific Reports*, 5,
828 p.14745, 2015.
- 829 Auerbach, L.W., Goodbred Jr, S.L., Mondal, D.R., Wilson, C.A., Ahmed, K.R., Roy, K., Steckler,
830 M.S., Small, C., Gilligan, J.M. and Ackerly, B.A. Flood risk of natural and embanked
831 landscapes on the Ganges-Brahmaputra tidal delta plain. *Nature Climate Change*, 5(2),
832 p.153, 2015.
- 833 Ayers, J. C., George, G., Fry, D., Benneyworth, L., Wilson, C., Auerbach, L., Roy, K., Karim, M.R.,
834 Akter, F., Goodbred, S. Salinization and arsenic contamination of surface water in
835 southwest Bangladesh. *Geochemical Transactions*, 18(1), 4, 2017.
- 836 Barua, D. K., Kuehl, S. A., Miller, R. L., & Moore, W. S. Suspended sediment distribution and
837 residual transport in the coastal ocean off the Ganges-Brahmaputra river
838 mouth. *Marine Geology*, 120(1-2), 41-61, 1994.
- 839 [Best, J. Anthropogenic stresses on the world's big rivers. *Nature Geoscience*, 12, pp 7-21,](#)
840 [doi: <https://doi.org/10.1038/s41561-018-0262-x>, 2019.](#)
- 841 Brammer, H. Bangladesh's dynamic coastal regions and sea-level rise. *Climate Risk*
842 *Management*, 1, pp.51-62, 2014.
- 843 Brown, J.M. and Davies, A.G. Flood/ebb tidal asymmetry in a shallow sandy estuary and the
844 impact on net sand transport. *Geomorphology*, 114(3), pp.431-439, 2010.
- 845 Brown, S. and Nicholls, R.J. Subsidence and human influences in mega deltas: the case of the
846 Ganges-Brahmaputra-Meghna. *Science of the Total Environment*, 527, pp.362-374,
847 2015.
- 848 Chatterjee, M., Shankar, D., Sen, G.K., Sanyal, P., Sundar, D., Michael, G.S., Chatterjee, A.,
849 Amol, P., Mukherjee, D., Suprit, K. and Mukherjee, A. Tidal variations in the Sundarbans
850 estuarine system, India. *Journal of Earth System Science*, 122(4), pp.899-933, 2013.

Deleted: review

Deleted: marine

Deleted: s

Deleted: reports

Deleted: earth

Deleted: system

Deleted: science

858 Darby, S.E., Hackney, C.R., Leyland, J., Kummu, M., Lauri, H. Parsons, D.R., Best, J.L, Nicholas,
859 A.P. and Aalto, R. Fluvial sediment supply to a mega-delta reduced by shifting tropical-
860 cyclone activity. *Nature*, 539, 276-279, doi:10.1038/nature19809, 2016.

861 Darby, S.E., Nicholls, R.J., Rahman, M.M., Brown, S. and Karim, R. A Sustainable Future
862 Supply of Fluvial Sediment for the Ganges-Brahmaputra Delta. In *Ecosystem Services for*
863 *Well-Being in Deltas* (pp. 277-291). Palgrave Macmillan, Cham, 2018.

864 Ericson, J.P., Vörösmarty, C.J., Dingman, S.L., Ward, L.G. and Meybeck, M. Effective sea-level
865 rise and deltas: causes of change and human dimension implications. *Global and*
866 *Planetary Change*, 50(1-2), pp.63-82, 2006.

867 Galloway, W.E. Process framework for describing the morphologic and stratigraphic
868 evolution of deltaic depositional systems in M.L. Broussard, ed. *Deltas: models for*
869 *exploration*, pp. 87-98, Houston Geological Society, 1975.

870 Goodbred Jr, S.L. and Kuehl, S.A. Holocene and modern sediment budgets for the Ganges-
871 Brahmaputra river system: Evidence for highstand dispersal to flood-plain, shelf, and
872 deep-sea depocenters. *Geology*, 27(6), pp.559-562, 1999.

873 Grinsted, A. Tidal fitting toolbox (v 1.3.0.0), Matlab code,
874 [https://www.mathworks.com/matlabcentral/fileexchange/19099-tidal-fitting-](https://www.mathworks.com/matlabcentral/fileexchange/19099-tidal-fitting-toolbox?s_tid=srchtitle)
875 [toolbox?s_tid=srchtitle](https://www.mathworks.com/matlabcentral/fileexchange/19099-tidal-fitting-toolbox?s_tid=srchtitle), 2008.

876 [Hanebuth, T.J.J., Kudrass, H.R., Linstadter, J., Islam, B., and Zander, A.M. Rapid coastal](#)
877 [subsidence in the central Ganges-Brahmaputra Delta \(Bangladesh\) since the 17th](#)
878 [century deduced from submerged salt-producing kilns. *Geology*, 41\(9\), pp.987-990,](#)
879 [2013.](#)

880 Higgins, S.A., Overeem, I., Steckler, M.S., Syvitski, J.P., Seeber, L. and Akhter, S.H. InSAR
881 measurements of compaction and subsidence in the Ganges-Brahmaputra Delta,
882 Bangladesh. *Journal of Geophysical Research: Earth Surface*, 119(8), pp.1768-1781,
883 2014.

884 Higgins, S., Overeem, I., Rogers, K. and Kalina, E. River linking in India: Downstream impacts
885 on water discharge and suspended sediment transport to deltas. *Elem Sci Anth*, 6(1),
886 2018.

887 Hossain, M.S., Dearing, J.A., Rahman, M.M, and Salehin, M. Recent changes in ecosystem
888 services and human well-being in the Bangladesh coastal zone. *Regional*
889 *Environmental Change* 16(2):429-443, 2016.

890 Islam, M.R. Managing Diverse Land Uses in Coastal Bangladesh: Institutional
891 Approaches. *Environment and livelihoods in tropical coastal zones*, p.237, 2006.

892 Kamal, A.S.M., Hossain, A., Hossain, B.M., Hassan, S.M. and Rashid, A.K.M. Physical and Social
893 Assessment of the Waterlogged Area and Suitability of the “Inclusive and Adaptive
894 Tidal River Management Technique” to Alleviate Waterlogging in Southwest
895 Bangladesh. *Procedia Engineering*, 212, pp.760-767. , 2018.

896 Khadim, F.K., Kar, K.K., Halder, P.K., Rahman, M.A. and Morshed, A.M. Integrated water
897 resources management (IWRM) impacts in south west coastal zone of Bangladesh and fact-
898 finding on tidal river management (TRM). *Journal of Water Resource and*
899 *Protection*, 5(10), p.953, 2013.

900 [Kudrass H.R., Michels K.H., Wiedicke M., Suckow A. Cyclones and tides as feeders of a](#)
901 [submarine canyon off Bangladesh. *Geology*, 26, pp.715-718, 1998.](#)

Formatted: Font: Italic

Deleted: 18

Deleted: engineering

904 [Kudrass, H.R., Machalett, B., Palamenghi, L., Meyer, I., and Zhang, W. Sediment transport by](#)
 905 [tropical cyclones recorded in a submarine canyon off Bangladesh. *Geo-Marine Letters*,](#)
 906 [38\(6\), pp.481-496.](#)
 907 [Lupker, M., France-Lanord, C., Lavé, J., Bouchez, J., Galy, V., Métivier, F., Gaillardet, J.,](#)
 908 [Lartiges, B., and Mugnier, J.L. A Rouse-based method to integrate the chemical](#)
 909 [composition of river sediments: Application to the Ganga basin. *Journal of Geophysical*](#)
 910 [Research: Earth Surface, 116, pp.1-24, 2011.](#)
 911 Marois, D.E. and Mitsch, W.J. Coastal protection from tsunamis and cyclones provided by
 912 mangrove wetlands—a review. *International Journal of Biodiversity Science, Ecosystem*
 913 *Services & Management*, 11(1), pp.71-83, 2015.
 914 Mcleod, E., Chmura, G.L., Bouillon, S., Salm, R., Björk, M., Duarte, C.M., Lovelock, C.E.,
 915 Schlesinger, W.H. and Silliman, B.R. A blueprint for blue carbon: toward an improved
 916 understanding of the role of vegetated coastal habitats in sequestering CO2. *Frontiers*
 917 *in Ecology and the Environment*, 9(10), pp.552-560, 2011.
 918 [Michels, K.H., Kudrass, H.R., and Hu, C. The submarine delta of the Ganges- Brahmaputra :](#)
 919 [cyclone-dominated sedimentation patterns. *Marine Geology*, 149, pp.133-154, 1998.](#)
 920 Nowreen, S., Jalal, M.R. and Khan, M.S.A. Historical analysis of rationalizing South West
 921 coastal polders of Bangladesh. *Water Policy*, 16(2), pp.264-279, 2014.
 922 Ogston, A.S. and Sternberg, R.W. Sediment-transport events on the northern California
 923 continental shelf. *Marine Geology*, 154(1-4), pp.69-82, 1999.
 924 Overeem I. and Syvitski, J.P.M. Dynamics and Vulnerability of Delta Systems: LOICZ Reports
 925 and Studies, No 35, GKSS Research Center, Geesthacht, 54 p., 2009.
 926 Pendleton, L., Donato, D.C., Murray, B.C., Crooks, S., Jenkins, W.A., Sifleet, S., Craft, C.,
 927 Fourqurean, J.W., Kauffman, J.B., Marbà, N. and Megonigal, P. Estimating global “blue
 928 carbon” emissions from conversion and degradation of vegetated coastal
 929 ecosystems. *PloS One*, 7(9), p.e43542, 2012.
 930 Pethick, J.S. Velocity surges and asymmetry in tidal channels. *Estuarine and Coastal Marine*
 931 *Science*, 11(3), pp.331-345, 1980.
 932 Pethick, J. and Orford, J.D. Rapid rise in effective sea-level in southwest Bangladesh: its
 933 causes and contemporary rates. *Global and Planetary Change*, 111, pp.237-245, 2013.
 934 Rinaldo, A., Fagherazzi, S., Lanzoni, S., Marani, M. and Dietrich, W.E. Tidal networks: 3.
 935 Landscape-forming discharges and studies in empirical geomorphic
 936 relationships. *Water Resources Research*, 35(12), pp.3919-3929, 1999.
 937 [Rogers, K.G., and Goodbred, S.L. Mass failures associated with the passage of a large tropical](#)
 938 [cyclone over the Swatch of No Ground submarine canyon \(Bay of Bengal\): *Geology*,](#)
 939 [38\(11\), pp.1051-1054, 2010.](#)
 940 Rogers, K.G., Goodbred Jr, S.L. and Mondal, D.R. Monsoon sedimentation on the ‘abandoned’
 941 tide-influenced Ganges–Brahmaputra delta plain. *Estuarine, Coastal and Shelf*
 942 *Science*, 131, pp.297-309, 2013.
 943 [Rogers, K.G., and Overeem, I. Doomed to drown? Sediment dynamics in the human-](#)
 944 [controlled floodplains of the active Bengal Delta. *Elementa: Science of the*](#)
 945 [Anthropocene](#), 6, p. 66. doi:10.1525/elementa.250, 2017.
 946 [Saha, M.K., and Khan, N. Changing profile of cyclones in the context of climate change and](#)
 947 [adaptation strategies in Bangladesh. *Journal of Bangladesh Institute of Planners*, 7, pp.](#)
 948 [63-78, 2014.](#)

Deleted: one

Formatted: Font: Not Italic

Formatted: Font: Not Italic

Formatted: Font: Not Italic

Formatted: Font: Italic

Formatted: Font: Not Italic

950 Sakib, M., Nihal, F., Haque, A., Rahman, M., & Ali, M. Sundarban as a Buffer against Storm
951 Surge Flooding. *World Journal of Engineering and Technology*, 3, 59–64, 2015.

952 Sarwar, M.G.M. and Woodroffe, C.D. Rates of shoreline change along the coast of
953 Bangladesh. *Journal of Coastal Conservation*, 17(3), pp.515-526, 2013.

954 [Seijger, C., Datta, D.K., Douven, W., van Halsema, G. and Khan, M.F. Rethinking sediments,
955 tidal rivers and delta livelihoods: tidal river management as a strategic innovation in
956 Bangladesh. *Water Policy*. doi: <https://doi.org/10.2166/wp.2018.212>, 2018.](#)

957 Shaha, D.C. and Cho, Y.K. Salt plug formation caused by decreased river discharge in a
958 multi-channel estuary. *Scientific Reports*, 6, p.27176, 2016.

959 [Shampa, M., and Pramanik, I.M. Tidal River Management \(TRM\) for Selected Coastal Area of
960 Bangladesh to Mitigate Drainage Congestion. *International Journal of Scientific and
961 Technology Research*, 1\(5\), pp.1–6, 2012.](#)

962 Steckler, M.S., Nooner, S.L., Akhter, S.H., Chowdhury, S.K., Bettadpur, S., Seeber, L. and
963 Kogan, M.G. Modeling Earth deformation from monsoonal flooding in Bangladesh using
964 hydrographic, GPS, and Gravity Recovery and Climate Experiment (GRACE)
965 data. *Journal of Geophysical Research: Solid Earth*, 115(B8), 2010.

966 Syvitski, J.P. Supply and flux of sediment along hydrological pathways: research for the 21st
967 century. *Global and Planetary Change*, 39(1-2), pp.1-11, 2003.

968 Syvitski, J.P. and Milliman, J.D. Geology, geography, and humans battle for dominance over
969 the delivery of fluvial sediment to the coastal ocean. *The Journal of Geology*, 115(1),
970 pp.1-19, 2007.

971 Syvitski, J.P. Deltas at risk. *Sustainability Science*, 3(1), pp.23-32, 2008.

972 Syvitski, J.P., Kettner, A.J., Overeem, I., Hutton, E.W., Hannon, M.T., Brakenridge, G.R., Day, J.,
973 Vörösmarty, C., Saito, Y., Giosan, L. and Nicholls, R.J. Sinking deltas due to human
974 activities. *Nature Geoscience*, 2(10), p.681, 2009.

975 Uddin, M. S., van Steveninck, E. D. R., Stuij, M., & Shah, M. A. R. Economic valuation of
976 provisioning and cultural services of a protected mangrove ecosystem: a case study on
977 Sundarbans Reserve Forest, Bangladesh. *Ecosystem Services*, 5, 88-93, 2013.

978 [van Staveren, M.F., Warner, J.F., Khan, M.S.A., and Shah Alam Khan, M. Bringing in the tides.
979 From closing down to opening up delta polders via Tidal River Management in the
980 southwest delta of Bangladesh. *Water Policy*, 19\(1\), pp.147–164, 2016.](#)

981 Wilson, C., Goodbred, S., Small, C., Gilligan, J., Sams, S., Mallick, B. and Hale, R. Widespread
982 infilling of tidal channels and navigable waterways in human-modified tidal delta plain
983 of southwest Bangladesh. *Elem Sci Anth*, 5, 2017.

984 Winterwerp, J.C. and Giardino, A. Assessment of increasing freshwater input on salinity and
985 sedimentation in the Gorai river system. *World Bank Project*, pp.1206292-000, 2012.

986 Yan, W. Can mangroves buffer ocean acidification?, *Eos*, 97, 2016.

987

988

989

990

991

Deleted: r

Formatted: Font: Not Italic

Formatted: Font: Italic

Formatted: Font: Not Italic

Deleted:

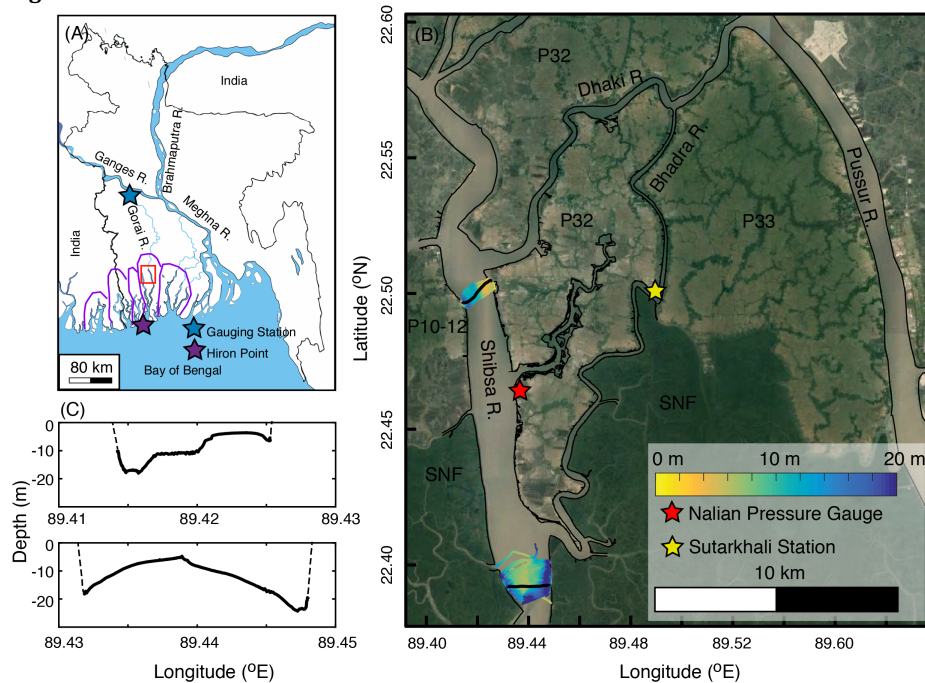
Formatted: Font: Italic

994 Table 1: Measurements of sediment flux and tidal prism from the Shibsra River. Shaded
 995 rows represent measurements taken during spring tides.
 996

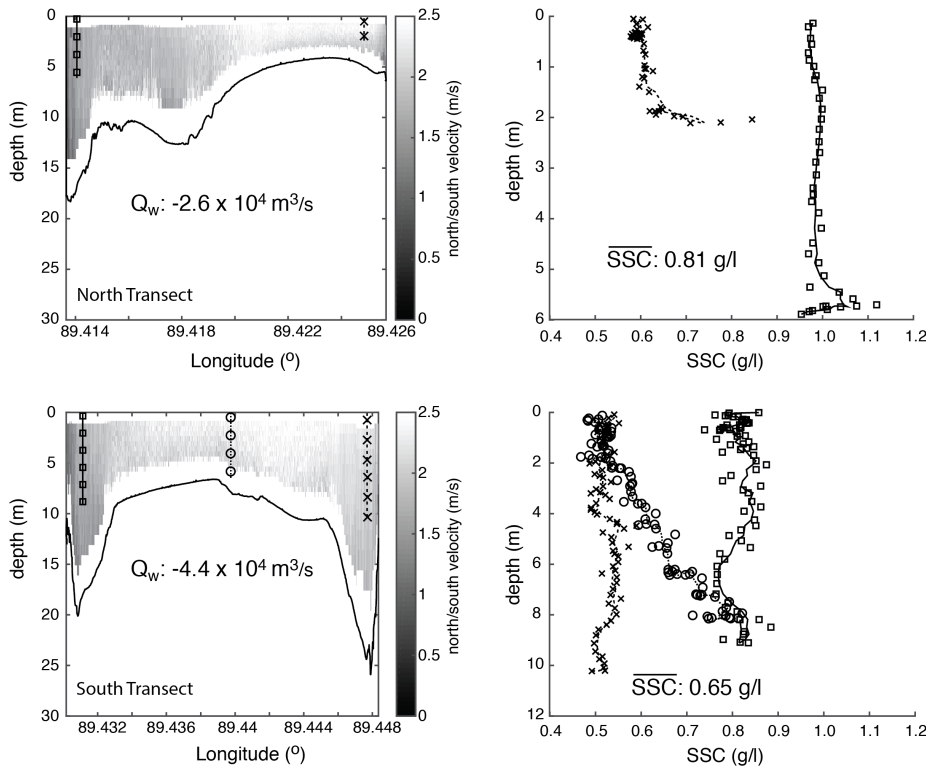
| | Transect | Tidal Range (m) | Tidal Prism (m ³) | | | Sediment Load (kg) | | |
|------------|----------|-----------------|-------------------------------|-----------|-----------|--------------------|-----------|-----------|
| | | | Ebb | Flood | Net | Ebb | Flood | Net |
| Dry Season | South | 2.1 | 2.00E+08 | -2.00E+08 | 4.30E+05 | 2.05E+07 | -4.70E+07 | -2.66E+07 |
| | North | 2.2 | 1.40E+08 | -1.50E+08 | -1.30E+07 | 1.55E+07 | -2.37E+07 | -8.21E+06 |
| | South | 5.5 | 4.50E+08 | -4.30E+08 | 2.30E+07 | 1.83E+08 | -2.30E+08 | -4.69E+07 |
| | North | 5.7 | 3.10E+08 | -2.30E+08 | 7.90E+07 | 2.15E+08 | -1.90E+08 | 2.49E+07 |
| Monsoon | South | 2.7 | 2.64E+08 | -1.81E+08 | 8.28E+07 | 4.47E+07 | -3.89E+07 | 5.77E+06 |
| | North | 2.2 | 1.83E+08 | -1.06E+08 | 7.69E+07 | 6.20E+07 | -4.12E+07 | 2.08E+07 |
| | South | 4 | 4.71E+08 | -5.12E+08 | -4.16E+07 | 3.20E+08 | -3.85E+08 | -6.50E+07 |
| | North | 3.9 | 2.40E+08 | -2.85E+08 | -4.43E+07 | 2.54E+08 | -3.31E+08 | -7.65E+07 |

997
 998
 999

1000 **Figures:**

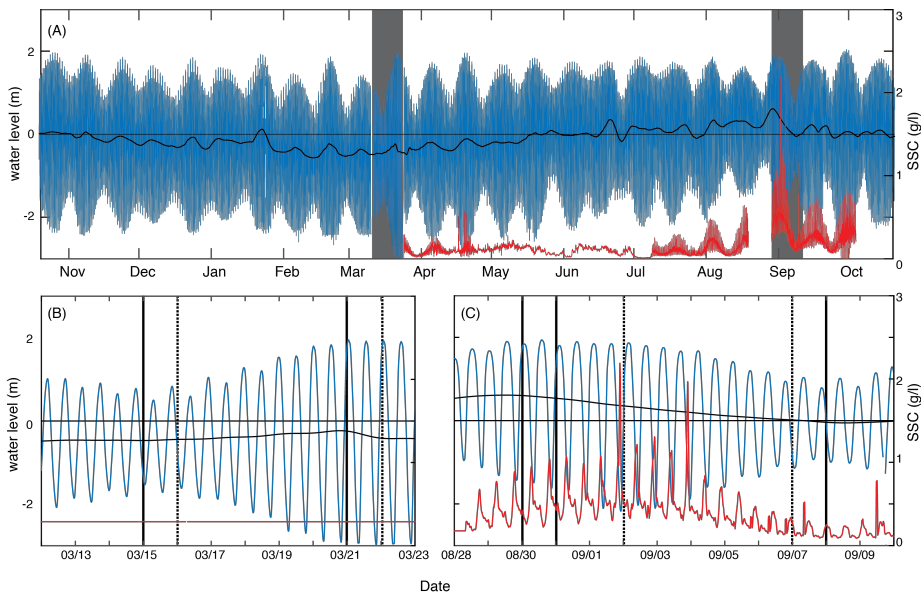


1001 Fig. 1 – A) Location of Bangladesh and the specific region of interest for this study, as well
1002 as the approximate outlines of the five major tidal distributary basins of the SW delta in
1003 purple. B) Satellite image of P-32 study area, with bathymetry overlain in the regions of the
1004 northern and southern transects. Long-term and short-term pressure sensor locations are
1005 also identified. C) Characteristic river cross sections for the northern and southern
1006 transects. The specific transects used for these cross sections are highlighted in black in
1007 (B).
1008



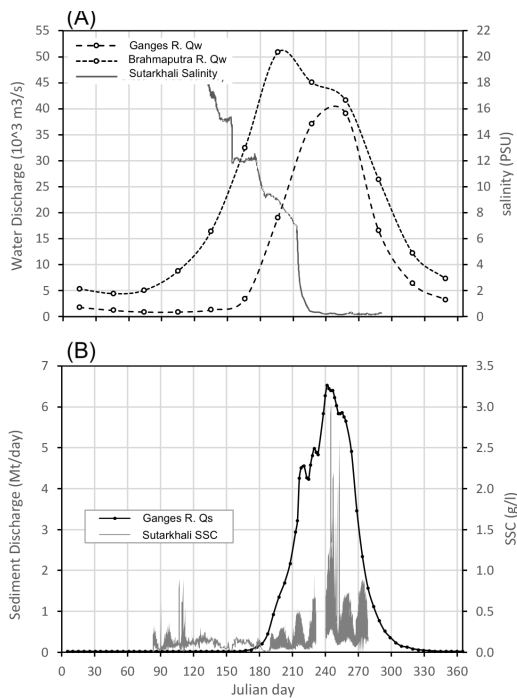
1009
1010
1011
1012
1013

Fig. 2 – Example channel cross sections of velocity and SSC collected near maximum ebb-oriented tides during the wet season at the north (top) and south (bottom) transects. Velocity measurements are spatially integrated to compute water discharge. SSC are averaged, with the product of velocity and SSC used to compute sediment discharge.



1014
 1015 **Fig. 3** – A) Long-term water level elevation (blue) and suspended sediment concentration
 1016 (red) recorded at Sutarkhali. Black is the tidally filtered water level to highlight seasonal
 1017 trends of relatively higher water during the monsoon, despite similar maximum tidal
 1018 elevation. Note also the arrival of increased SSC associated with monsoon discharge of the
 1019 GBM, beginning in August. Areas shaded in gray depict the periods of focused field work,
 1020 highlighted below in panels (B) and (C). Days where transect measurements were recorded
 1021 are noted with vertical black lines, where solid are from the southern transect, and dashed
 1022 are from the northern transect. In (B), the horizontal red line represents the maximum SSC
 1023 observed in the spring-neap tidal cycle following our focused field work, as SSC was not
 1024 measured at this location previously.

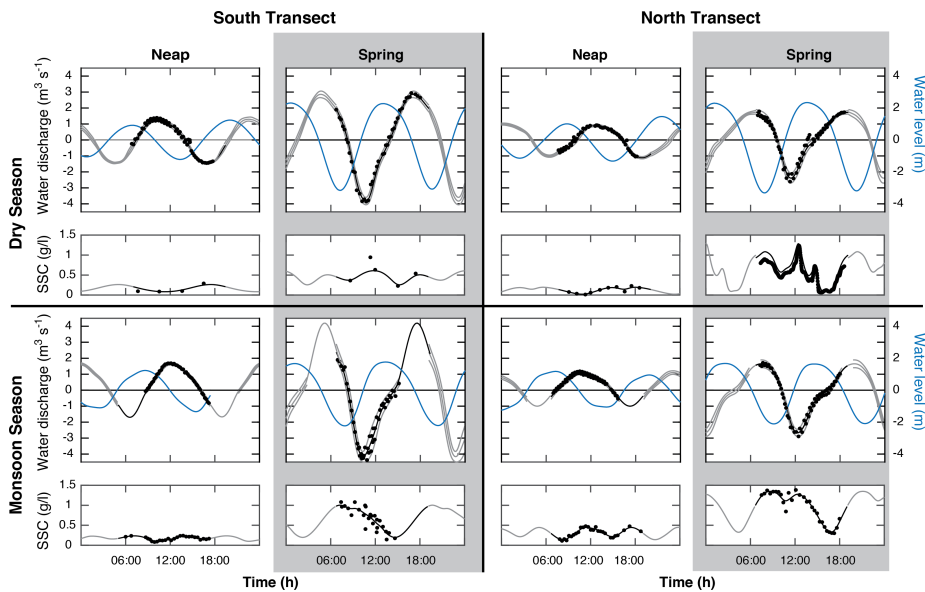
Deleted: Fig. 2



1026
1027
1028
1029
1030
1031

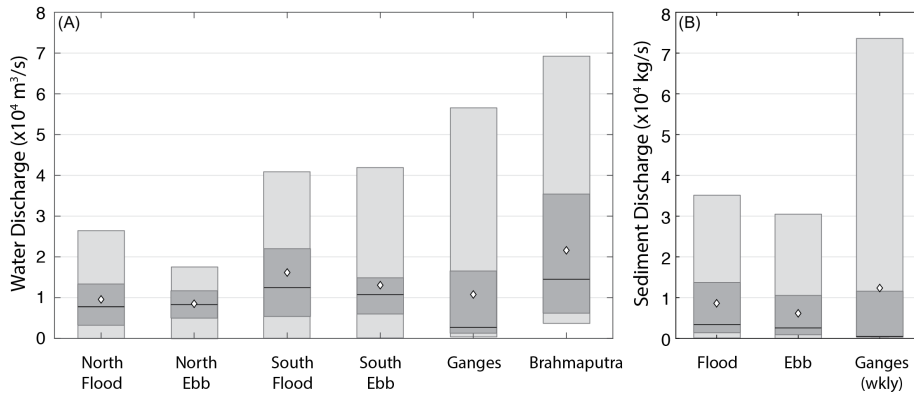
Fig. 4 – A) Ganges and Brahmaputra River water discharge (Q_w), and salinity measured at Sutarkhali Station, demonstrating the reduction in P-32 salinity associated with the arrival of freshwater from the GBM rivers. B) Ganges river sediment discharge (Q_s) [interpolated from Lupker et al. \(2011\)](#) and SSC measured at Sutarkhali station, demonstrating the increase in local SSC coincident with the peak SSC discharge of the Ganges R.

Deleted: Fig. 3



1033
 1034 **Fig. 5** - Instantaneous water discharge, water level, and depth and width-averaged SSC for
 1035 each day of cross-channel transects. Dry season measurements are in the upper half, while
 1036 monsoon season transects are on the bottom. Spring tides in either season are shaded in
 1037 gray. The two left columns are southern measurements, and the two right columns are
 1038 from the northern transect. Black dots correspond to specific measurements, while gray
 1039 lines represent the estimated error, tile forwards and backwards by 12.4 hours. For
 1040 discharge, dashed lines in the monsoon represent maxima based on extrapolations from
 1041 the dry season ratio. While seemingly unreasonable, they are provided here for context.
 1042
 1043
 1044

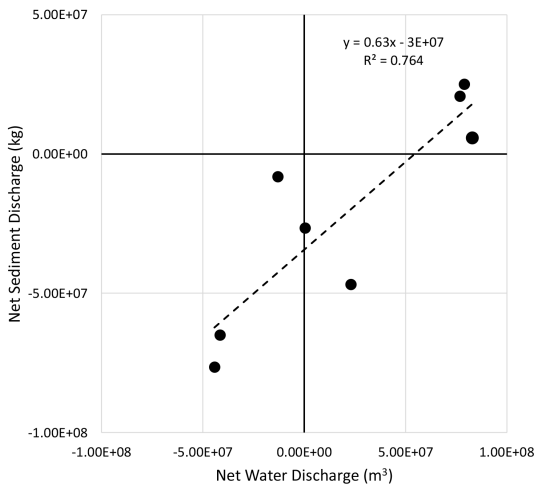
Deleted: Fig. 4



1046
1047
1048
1049
1050
1051
1052
1053

Fig. 6 – Comparison of mean (diamond), median (black line), 25th and 75th percentile (lower and upper limits of darkly shaded box) and total range (lightly shaded box) for water discharge (A), and sediment discharge (B). A) demonstrates that median and mean discharge along either transect are comparable to those of either the Ganges or Brahmaputra River. B) demonstrates that as with water, mean sediment discharge on both the flood and ebb tides is approximately the same as the weekly averaged Ganges sediment discharge.

Deleted: Fig. 5



1054
1055
1056
1057
1058

Fig. 7 – Net water discharge vs. net sediment discharge for all of the survey days on the Shibsra River. As expected, we observe a positive trend to this relationship. The negative y-intercept of the best-fit curve demonstrates the overall flood-oriented nature of sediment transport in this tidal channel.

Deleted: Fig. 6